

Planar Herding of Multiple Evaders by a Single Pursuer

Rishabh Kumar Singh and Debraj Chakraborty

Abstract—In this paper, a planar herding problem is addressed, where a single superior pursuer herds a flock of non-cooperative, inferior evaders around a predefined target point. An inverse square law of repulsion is assumed between the pursuer and each evader. It is demonstrated that a constant-velocity, circular trajectory of the pursuer, encompassing all the evaders and centered around the target point, guarantees the herding of the evaders into an arbitrarily small limit cycle around the target point. The conditions for the stability of this limit cycle, as well as the radius of the limiting herd, are derived as functions of the pursuer's radius, angular velocity, and the strength of pursuer-evader repulsion. Estimates of the region of attraction for this stable limit cycle are computed and are found to lie within a larger unstable limit cycle, which is itself contained within the pursuer's trajectory.

I. INTRODUCTION

Multiple-evader versus single-pursuer differential games have direct applications across a wide range of scientific domains, including robotics [1], behavioral science [2], wildlife control [3], search and rescue [4], crowd control [5], and military applications [6]. In many such scenarios, the evaders are non-cooperative and resist being herded together, while they are repelled by the presence of the pursuer. Conversely, the pursuer is faster than the evaders and aims to gather or herd all of them into a target set. Although several attempts have been made in the literature to understand, simulate, and analyze such games and strategies (e.g. see [7] and the references therein), no formal solutions have yet been established. In this paper, we propose an extremely simple yet effective strategy for the pursuer that guarantees successful herding for any number of evaders, assuming an inverse square law of repulsion. The initial investigation into the herding problem was inspired by several naturally occurring herding phenomena, such as sheepdogs herding flocks of sheep [1], [8], [9], [10] and predator-prey interactions [11], [12], [13]. Most of these early works were based on mathematical models designed to replicate herding behavior in extensive simulations, with little or no emphasis on theoretical analysis. Subsequently, the complexity of analyzing multiple evaders simultaneously has proven to be a bottleneck in developing a comprehensive theory for such games. Conversely, the problem of herding a single evader by a pursuer has been satisfactorily solved through multiple approaches [14], [15], [16]. Meanwhile, a body of research focused on modeling and simulating scenarios involving multiple pursuers herding a group of evaders has also developed [17], [18], [19] [20]. The synthesis of controllers with provable convergence

properties was introduced in [21], where a sliding mode controller was proposed to herd a single evader using a group of pursuers along a desired trajectory. An arc-based approach was employed in [19] to herd multiple evaders with multiple pursuers. In contrast to the simpler formulations mentioned earlier, the more complex problem of herding multiple evaders with a single pursuer was investigated in [22], [23], and [24], where variants of switched sliding mode controllers were proposed. However, the solutions provided rely on the crucial assumption of non-uniform repulsion between the pursuer and the "chased" and "unchased" evaders. The slower reaction of the unchased evader allows for the sequential collection of all evaders at the target through a switched control approach. In both natural and robotic herding situations, however, it is often difficult for an individual evader to determine whether and when it is being specifically "chased." Generally, most researchers have modeled repulsion based solely on the instantaneous distance from the pursuer [7]. A key difference in our work, compared to the majority of naturally inspired herding models reviewed above, is the absence of attraction between the evaders. While this makes herding more challenging, we believe it is justified in most engineering applications. Specifically, our interaction model is similar to that in [19], although we demonstrate that herding is possible for such models with just one (sufficiently capable) pursuer.

In this paper, we propose a simple yet effective strategy for a single pursuer to herd multiple evaders around a predefined target point. The proposed strategy assumes that all evaders are initially enclosed within a circle centered at the target point, with the pursuer positioned on the circumference (see Fig. 1). Let the radius of this circle, referred to as the "pursuer circle" throughout the paper, be denoted as R . The pursuer's policy involves moving around the target point along this circle with a constant angular velocity ω . We show that

- 1) If ω and/or R are sufficiently large with respect to the repulsion between the evader and pursuer, then two circular equilibria/limit cycles gets created for the evaders around the target point (see figure 2).
- 2) The outer limit cycle (denoted by the red circle with radius r_1^* in figure 2) is unstable, while the inner one (blue with radius r_2^*) is stable.
- 3) By increasing the pursuer's angular velocity, the radius of the inner stable limit cycle can be made arbitrarily small, while the outer unstable limit cycle approaches the pursuer circle.
- 4) The evaders' rate of convergence to the stable limit

The authors are with the Department of Electrical Engineering, Indian Institute of Technology Bombay, Mumbai, Maharashtra, India. Email: 214070024@iitb.ac.in, dc@ee.iitb.ac.in

1) *Evader Kinematics in $\{r, \phi\}$ -frame:* We temporarily drop the subscript i , denoting the evader number, to simplify notation. Using (2) in (1) and converting it into polar coordinates, the (i -th) evader coordinates $\{r = \sqrt{x_{e_i}^2 + y_{e_i}^2}, \phi = \tan^{-1} \frac{y_{e_i}}{x_{e_i}}\}$ satisfies:

$$\begin{aligned} \dot{r}(t) &= \frac{k(r(t) - R \cos(\phi(t) - \omega t))}{(r^2(t) + R^2 - 2r(t)R \cos(\phi(t) - \omega t))^{\frac{3}{2}}} \\ \dot{\phi}(t) &= \frac{kR \sin(\phi(t) - \omega t)}{r(t)(r^2(t) + R^2 - 2r(t)R \cos(\phi(t) - \omega t))^{\frac{3}{2}}} \end{aligned} \quad (3)$$

Clearly these equations represent a time-varying system. To simplify analysis, we change coordinates again to obtain the following.

2) *Evader Kinematics in $\{r, \psi\}$ -frame:* Define $\psi(t) := \phi(t) - \omega t$ and replace in (3), thereby simplifying it to a time-invariant form:

$$\begin{aligned} \dot{r}(t) &= \frac{k(r(t) - R \cos(\psi(t)))}{(r^2(t) + R^2 - 2r(t)R \cos(\psi(t)))^{\frac{3}{2}}} \\ \dot{\psi}(t) &= \frac{kR \sin(\psi(t))}{r(t)(r^2(t) + R^2 - 2r(t)R \cos(\psi(t)))^{\frac{3}{2}}} - \omega. \end{aligned} \quad (4)$$

3) *Evader Kinematics in $\{u, v\}$ -frame:* Though (4) will prove to be convenient enough for analysis purposes, polar frames are inconvenient for visualization. Hence we compute the equivalent system of (4) in the Cartesian $\{u, v\}$ -frame:

$$\begin{aligned} \dot{u}(t) &= \frac{k(u(t) - R)}{((u(t) - R)^2 + v^2(t))^{\frac{3}{2}}} + \omega v(t) \\ \dot{v}(t) &= \frac{k(v(t))}{((u(t) - R)^2 + v^2(t))^{\frac{3}{2}}} - \omega u(t) \end{aligned} \quad (5)$$

III. HERDING OF SINGLE EVADER

In this section we will analyze the behaviour of (3), (4) or (5). Specifically, we will evaluate whether the proposed pursuer strategy given by (2) is effective for a single evader. The case of multiple evaders will be considered in the following section.

A. Equilibrium points

The equilibrium point of (4) is most convenient to calculate. Indeed setting $\dot{r}(t) = 0$ and $\dot{\psi}(t) = 0$, we get (denoting (r^*, ψ^*) as the equilibrium point):

$$\begin{aligned} r^* &= R \cos(\psi^*) \\ \omega &= \frac{kR \sin(\psi^*)}{r^* [(r^*)^2 + R^2 - 2r^*R \cos(\psi^*)]^{\frac{3}{2}}} \end{aligned} \quad (6)$$

Eliminating r^* from the above equations, we get

$$\cos(\psi^*) \sin^2(\psi^*) = \frac{k}{\omega R^3}. \quad (7)$$

1) *Existence of Equilibrium Points:* We know that $-0.385 < \cos(\psi^*) \sin^2(\psi^*) < 0.385$ and k, ω and R are all positive, which implies $0 < \frac{k}{\omega R^3} < 0.385$. Hence if and only if, this inequality is satisfied by k, ω and R , there exists equilibrium points (r^*, ψ^*) for (4). The next lemma follows immediately.

Lemma 2. *System (4) has equilibrium points if and only if $0 < \frac{k}{\omega R^3} < 0.385$. Equivalently, system (3) has limit sets/cycles if and only if $0 < \frac{k}{\omega R^3} < 0.385$.*

2) *Computation of Equilibrium Points:* Eliminating ψ^* from (6) and (7), we get

$$r^{*3} - R^2 r^* + \frac{k}{\omega} = 0 \quad (8)$$

Denote the three roots of (8) by r_1^*, r_2^* and r_3^* . Note that $\frac{k}{\omega R^3} < 0.385 \implies \frac{-R^6}{27} + \frac{k^2}{4\omega^2} < 0$. From the theory of general cubic equation [25], this implies that all the roots

are real. If we denote $\sigma_1 = \left(-\sqrt{\frac{k^2}{4\omega^2} - \frac{R^6}{27}} - \frac{k}{2\omega}\right)^{\frac{1}{3}}$ and $\sigma_2 = \left(\sqrt{\frac{k^2}{4\omega^2} - \frac{R^6}{27}} - \frac{k}{2\omega}\right)^{\frac{1}{3}}$ then

$$\begin{aligned} r_1^* &= \sigma_2 + \sigma_1 \\ r_2^* &= \frac{-\sigma_2}{2} + \frac{\sqrt{3}\sigma_1}{2}j - \frac{\sigma_1}{2} - \frac{\sqrt{3}\sigma_2}{2}j \\ r_3^* &= \frac{-\sigma_2}{2} - \frac{\sqrt{3}\sigma_1}{2}j - \frac{\sigma_1}{2} + \frac{\sqrt{3}\sigma_2}{2}j \end{aligned} \quad (9)$$

Lemma 3. *For $\frac{k}{\omega R^3} < 0.385$ and for finite k, ω and R , the three roots (9) satisfy $R > r_1^* > \frac{R}{\sqrt{3}} > r_2^* > 0 > r_3^*$.*

Clearly, the negative root r_3^* is not relevant to our analysis since radius must be positive. The other roots r_1^*, r_2^* each correspond to an equilibrium point for (4). The corresponding angles are $\psi_1^* = \cos^{-1} \frac{r_1^*}{R}$ and $\psi_2^* = \cos^{-1} \frac{r_2^*}{R}$. In Fig. 2, these two equilibrium points are depicted in the $\{u, v\}$ -frame with the red and blue dots respectively. In the next result, we analyze the effect of increasing ω on the location of the equilibrium points.

Lemma 4. *For system (4), and the equilibrium radii defined as in (9), $r_2^* \rightarrow 0$ and $r_1^* \rightarrow R$ as $\omega \rightarrow \infty$.*

B. Stability of equilibrium points

Theorem 5. *For the system described in (4), let $0 < \frac{k}{\omega R^3} < 0.385$, and $(r_1^*, \psi_1^*), (r_2^*, \psi_2^*)$ be the equilibrium points defined in (9) and Lemma 3. Then*

- 1) (r_2^*, ψ_2^*) is asymptotically stable
- 2) (r_1^*, ψ_1^*) is a saddle point

C. Estimation of the Region of Attraction of (r_2^*, ψ_2^*)

Since the asymptotic stability of (r_2^*, ψ_2^*) has already been established, we aim to estimate a maximal region of attraction. A good estimate will also test the effectiveness of the proposed strategy. For this purpose, we first denote (r_2^*, ψ_2^*) in the cartesian $\{u, v\}$ -frame as $u^* = r_2^* \cos \psi_2^*$ and $v^* = r_2^* \sin \psi_2^*$. The equations of motion in this frame were already derived in (5). For computational purposes,

we further shift the origin of the $\{u, v\}$ -frame to $\{u^*, v^*\}$. Denote this new frame as $\{\bar{u} = u - u^*, \bar{v} = v - v^*\}$, and the equations are modified to:

$$\begin{aligned}\dot{\bar{u}} &= \frac{k(\bar{u} - R + u^*)}{((\bar{u} - R + u^*)^2 + (\bar{v} + v^*)^2)^{\frac{3}{2}}} + \omega(\bar{v} + v^*), \\ \dot{\bar{v}} &= \frac{k(\bar{v} + v^*)}{((\bar{u} - R + u^*)^2 + (\bar{v} + v^*)^2)^{\frac{3}{2}}} - \omega(\bar{u} + u^*).\end{aligned}\quad (10)$$

Definition 1. [26] Define $w = [\bar{u}, \bar{v}]^T$, denote (10) as $\dot{w} = f(w)$ and $\psi(t; w_0)$ as the solution starting at $t = 0$ from $w(0) = w_0$. For the asymptotically stable equilibrium point $w^* = \mathbf{0}$, the associated region of attraction is defined as:

$$R_A = \{w_0 \in \mathbb{R}^2 \mid \psi(t; w_0) \rightarrow 0 \text{ as } t \rightarrow \infty\} \quad (11)$$

We use a computational method proposed in [27] to find a quadratic estimate of the region of attraction (ROA) for this system. The method is restricted to identifying an ellipsoidal region, where the area is maximized to create the best inner approximation for R_A . We briefly review this method below.

The method consists of creating a Lyapunov function $V(w) = w^T \hat{A} w$, $\hat{A} = \hat{A}^T > 0$ and approximating R_A by the set $\bar{\Omega} = \{w \in \mathbb{R}^2 : V(w) \leq c\}$. The functional V must satisfy the standard Lyapunov function properties $V(w) > 0, \forall w \in \bar{\Omega}, V(0) = 0, \dot{V}(w) < 0, \forall w \in \bar{\Omega}, \dot{V}(0) = 0$. We aim to find the ellipse with the largest area, which can then be used as the proposed approximation of R_A . Therefore, the goal is to determine \hat{A} and c so that area contained in closed surface $w^T \hat{A} w = c$ is maximized. We can normalize this equation and write as follows:

$$w^T A w = 1 \quad (12)$$

where $A = \frac{\hat{A}}{c}$. Clearly, the area contained in the closed curve (12).

$$\text{Area} \propto \frac{1}{\lambda_1(A)\lambda_2(A)}$$

where $\lambda_1(A)$ and $\lambda_2(A)$ are the eigenvalues of A . Also $\dot{V}(w) = 2\dot{w}Aw$. Hence the requirement of $\dot{V}(w) < 0, \forall w \in \bar{\Omega}$ translates to $f^T(w)Aw < 0 \forall w \in \bar{\Omega}$. Hence the following optimization problem can be formulated:

Problem 6. $\min_{A \in \mathbb{R}^{2 \times 2}} \prod_{i=1}^2 \lambda_i(A)$ such that

- 1) $\lambda_i(A) > 0, \forall i = 1, 2$
- 2) $f^T(w)Aw < 0, \forall w \in \bar{\Omega} := \{w \mid w^T A w \leq 1, w \neq 0\}$

Unlike in [26], we use a modern constrained optimization routine (e.g. `fmincon` in MATLAB [28]) to obtain solutions of problem 1. The initial guess for the A matrix is taken to be the normalized solution of the Lyapunov equation $AJ + J^T A = -\mathbf{I}$, where J is the Jacobian of (10) evaluated at the stable equilibrium point ($\bar{u} = 0, \bar{v} = 0$).

For notational convenience, let the set $\bar{\Omega}$ shifted back to the $\{u, v\}$ frame, be denoted by Ω . Two instances of Ω are shown in Fig. 3 in a two separate $\{u, v\}$ frame.

Remark 7. Note that the ROA is plotted in the $\{u, v\}/\{r, \psi\}$ frame. However, In the $\{x, y\}/\{r, \phi\}$ frame, the ROA depends on the initial position of the pursuer. This will be discussed in the next section.

D. Translation of Results to $\{x, y\}/\{r, \phi\}$ -frame

Sections III-A, III-B, and III-C dealt almost entirely in the $\{u, v\}/\{r, \psi\}$ frame, mainly due to the time-invariance of the system equations in this frame. However we need to interpret all the results in the $\{x, y\}/\{r, \phi\}$ frame for physical understanding of the solution. In all the results below we simply use the fact that the solutions $r(t)$ remains the same in both $\{u, v\}$ and $\{x, y\}$ frame. On the other hand, any $\psi(t)$ in the $\{u, v\}$ frame translates to $\phi(t) = \psi(t) + \omega(t)$ in the $\{x, y\}$ frame.

1) Equilibrium sets/limit cycles:

Theorem 8. Consider system (3). If $\frac{k}{\omega R^3} < 0.385$, then (3) has two limit cycles inside D_z^R .

- 1) The first limit cycle is described by the trajectory $L_2 := \{r_2^*(t) = r_2^*, \phi_2^*(t) = \psi_2^* + \omega t, \forall t \geq 0\}$.
- 2) L_2 is asymptotically stable.
- 3) The second limit cycle is described by the trajectory $L_1 := \{r_1^*(t) = r_1^*, \psi_1^*(t) = \psi_1^* + \omega t, \forall t \geq 0\}$.
- 4) L_1 is unstable.

Proof: The proof follows directly from lemma 2, 3 and theorem 5.

The next result shows that the evader can be driven arbitrarily close to the target by choosing a sufficiently large pursuer velocity.

Corollary 9. For any $\epsilon > 0, \exists W > 0$ such that if $\omega > W$, then the radius of L_2 i.e. $r_2^* < \epsilon$

Proof: The proof follows from lemma 4.

2) *ROA in $\{x, y\}$ frame:* Clearly, (4) is a time-varying system, and thus, the region of attraction must be re-defined. Note, however, that the set of points converging to the stable limit cycle changes with time in the $\{x, y\}$ frame, while this set is invariant in the $\{u, v\}$ frame. A moment's reflection reveals that both the actual ROA, R_A , and our ellipsoidal approximation, Ω , are actually rotating around the origin in the $\{x, y\}$ frame at a constant angular velocity ω . Two snapshots of this rotation of Ω are shown in Fig. 3. It is evident that the ROA depends on the instantaneous orientation of the $\{u, v\}$ frame (denoted by θ in Fig. 3), which in turn depends on the relative position of the pursuer. To address this $\{u, v\}$ dependence, we refine the notation of ROA in section III-C to $R_A(\theta)$, and $\Omega(\theta)$, to denote the ROA and its approximation in the particular $\{u, v\}$ frame rotated by angle θ from the $\{x, y\}$ frame (see Fig. 3).

Based on the above discussion, an appropriate notion of ROA in this case can be defined as follows. Let the position of the pursuer in the $\{x, y\}$ frame be denoted by P , and let the boundary of D_z^R be represented as ∂D_z^R . Denote the solution of system (1) (dropping the subscript i) corresponding to initial evader position $\{x_0, y_0\}$ and initial pursuer position $\{P_0\}$, as $\phi(t; x_0, y_0, P_0)$. Note that the

$\phi(t; x_0, y_0, P_0)$ is expected to converge onto the stable limit cycle L_2 .

Definition 2. The ROA of the limit set L_2 is defined as: $R_A^{\{x,y\}} = \{\{x_0, y_0\} \in \mathbb{R}^2 | \phi(t; x_0, y_0, P_0) \rightarrow L_2 \text{ as } t \rightarrow \infty, \forall P_0 \in \partial D_z^R\}$

Clearly, $R_A^{\{x,y\}} = \bigcap_{\theta \in \{0, 2\pi\}} R_A(\theta)$ and a simple approximation (though possibly conservative) of $R_A^{\{x,y\}}$ can be computed by the intersection:

$$\Omega^{\{x,y\}} = \bigcap_{\theta \in \{0, 2\pi\}} \Omega(\theta)$$

An example of this intersection for $R = 2, k = 1$ and $\omega = 1$ is plotted in Fig.4, where the pink circle encompasses $\Omega^{\{x,y\}}$. Evidently, any evader with initial position within $\Omega^{\{x,y\}}$ converges to L_2 as $t \rightarrow \infty$ regardless of the initial position of the pursuer within D_z^R .

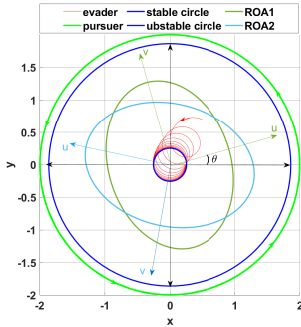


Fig. 3: Rotated ROA in static frame

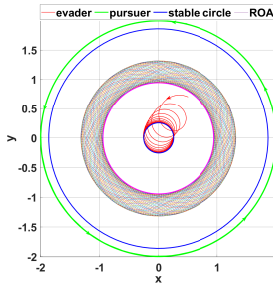


Fig. 4: Intersection of all ROA represents a circle in static frame

IV. HERDING OF MULTIPLE EVADER

In this section, we demonstrate that problem 1 can be solved using the strategy proposed in section II-B. While herding multiple evaders around a target with a single pursuer may initially seem more challenging than guiding a single evader to the target, we observe that the entire stability analysis from section III is independent of the specific position of each evader e_i as long as $\{x_{e_i}(0), y_{e_i}(0)\} \in \Omega^{\{x,y\}}$. In fact in the $\{r, \psi\}$ frame, the following result is self-evident.

Theorem 10. Consider the representation of the motion of the i^{th} evader ($i = 1, \dots, n$) in the $\{r, \psi\}$ frame (i.e. (4) with

$\{r, \psi\}$ replaced with $\{r_i, \psi_i\}$). Then, if $0 < \frac{k}{\omega R^3} < 0.385$, the following results hold:

- 1) Each evader has two equilibrium points (r_1^*, ψ_1^*) and (r_2^*, ψ_2^*) satisfying $R > r_1^* > \frac{R}{\sqrt{3}} > r_2^* > 0$. Corresponding $\psi_1^* = \cos^{-1}(\frac{r_1^*}{R})$ and $\psi_2^* = \cos^{-1}(\frac{r_2^*}{R})$.
- 2) The equilibrium point $\{r_2^*, \psi_2^*\}$ is asymptotically stable for each evader.
- 3) The equilibrium point $\{r_1^*, \psi_1^*\}$ is a saddle point for each evader.
- 4) For any $\epsilon > 0, \exists W > 0$ such that if $\omega > W$ then $r_2^* < \epsilon$.

Clearly the computation of the ROA is independent of the evader index and hence it is guaranteed that if $\{u_i(0), v_i(0)\} \in R_A \forall i = 1, \dots, n$ then each $u_i(t) \rightarrow u_2^* = r_2^* \sin(\psi_2^*)$ and $v_i(t) \rightarrow v_2^* = r_2^* \cos(\psi_2^*)$ as $t \rightarrow \infty$. In the $\{x, y\}$ frame, equivalently theorem 8 holds for each evader, as does the computation of the interested ROA, $\Omega^{\{x,y\}}$. Ultimately, the insensitivity to the evader index 'i' for all these results imply:

Theorem 11. If $0 < \frac{k}{\omega R^3} < 0.385$, and if $\{x_{e_i}, y_{e_i}\} \in \Omega^{\{x,y\}} \forall i = 1, \dots, n$ then under the pursuer strategy (2), each evader converges asymptotically onto the limit cycle L_2 (as defined in theorem 8). Moreover, ω can be chosen to arbitrarily reduce the radius of L_2 .

The following section illustrate the above result with typical convergent trajectory in various reference frames.

V. SIMULATION RESULTS

Simulation results are shown for both single and multiple evader situations.

A. For single evader

Figs. 5a and 5b depict the behavior of an evader when $R = 2, k = 1$ with $\omega = 1$ and $\omega = 0.5$, respectively. We observe that the path of the evader's trajectory forms a spiral as it approaches the limit set, which is a circle with radius r_2^* . Comparing these two figures, it is clear that ω is inversely related to the radius r_2^* of the limit set L_2 as expected from lemma 4.

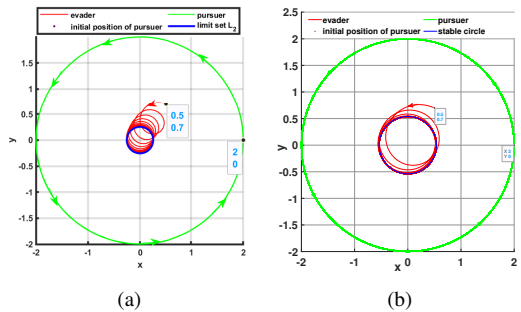


Fig. 5: Evader and pursuer trajectory in $\{x, y\}$ coordinate frame for (a): $R = 2, \omega = 1, k = 1, r_2^* = 0.25$, (b): $R = 2, \omega = 0.5, k = 1, r_2^* = 0.53$

Figs. 6a and 6b show the corresponding evader trajectories in the $\{r, \psi\}/\{u, v\}$ frame, where the evader converges to the equilibrium point (r_2^*, ψ_2^*) . The effect of decreasing ω is evident from the reduced frequency of the spiral in Fig. 6b.

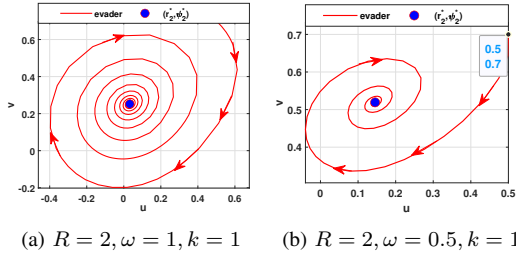


Fig. 6: Evader trajectory in $\{r, \psi\}$ frame

B. Multiple evaders

In the case of multiple (three) evaders, shown in Fig. 7a, all three evaders asymptotically converge onto the limit set L_2 in the $\{x, y\}/\{r, \phi\}$ frame.

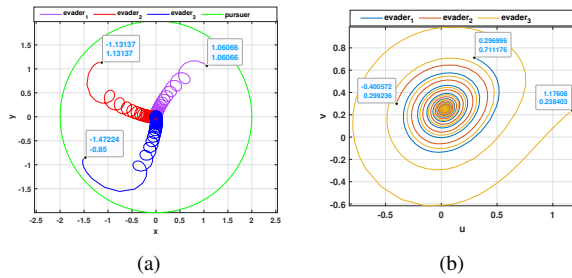


Fig. 7: Evader and pursuer trajectory in (a): $\{x, y\}$ coordinate frame, (b): rotating frame for $R = 2, \omega = 2, k = 1$

Fig. 7b shows the corresponding evader trajectories in the $\{u, v\}/\{r, \psi\}$ coordinate frame, where all evaders converge to the common equilibrium point $(r_2^*, \psi_2^*) = (0.2541, 1.4434)$, regardless of the initial positions.

VI. CONCLUSION

This paper proposes a simple strategy for herding a group of evaders using a single pursuer. The resulting motion is analyzed and the stability and the region of attraction of the limiting herd are studied. It is shown that the pursuer's angular velocity and distance from the target can be adjusted to achieve an arbitrarily small herd radius and faster convergence. Future research could explore theoretical estimates of the ROA and investigate alternative pursuer strategies based on the concepts developed here.

REFERENCES

- [1] R. Vaughan, N. Sumpter, J. Henderson, A. Frost, and S. Cameron, "Experiments in automatic flock control," *Robotics and autonomous systems*, vol. 31, no. 1-2, pp. 109–117, 2000.
- [2] A. J. Wood and G. J. Ackland, "Evolving the selfish herd: emergence of distinct aggregating strategies in an individual-based model," *Proceedings of the Royal Society B: Biological Sciences*, vol. 274, no. 1618, pp. 1637–1642, 2007.
- [3] "helicopter cowboys of australia's outbackâ," <https://www.bbc.com/news/world-asia-pacific-12408888>.

- [4] S. Van Havermaet, P. Simoens, T. Landgraf, and Y. Khaluf, "Steering herds away from dangers in dynamic environments," *Royal Society Open Science*, vol. 10, no. 5, p. 230015, 2023.
- [5] R. L. Hughes, "The flow of human crowds," *Annual review of fluid mechanics*, vol. 35, no. 1, pp. 169–182, 2003.
- [6] V. S. Chipade, V. S. A. Marella, and D. Panagou, "Aerial swarm defense by stringnet herding: Theory and experiments," *Frontiers in Robotics and AI*, vol. 8, p. 640446, 2021.
- [7] N. K. Long, K. Sammut, D. Sgarioto, M. Garratt, and H. A. Abbass, "A comprehensive review of shepherding as a bio-inspired swarm-robotics guidance approach," *IEEE Transactions on Emerging Topics in Computational Intelligence*, vol. 4, no. 4, pp. 523–537, 2020.
- [8] J.-M. Lien, O. B. Bayazit, R. T. Sowell, S. Rodriguez, and N. M. Amato, "Shepherding behaviors," in *IEEE International Conference on Robotics and Automation, 2004. Proceedings. ICRA'04. 2004*, vol. 4. IEEE, 2004, pp. 4159–4164.
- [9] T. Miki and T. Nakamura, "An effective simple shepherding algorithm suitable for implementation to a multi-mmobile robot system," in *First International Conference on Innovative Computing, Information and Control-Volume I (ICIC'06)*, vol. 3. IEEE, 2006, pp. 161–165.
- [10] D. Strömbom, R. P. Mann, A. M. Wilson, S. Hailes, A. J. Morton, D. J. Sumpter, and A. J. King, "Solving the shepherding problem: heuristics for herding autonomous, interacting agents," *Journal of the royal society interface*, vol. 11, no. 100, p. 20140719, 2014.
- [11] W. D. Hamilton, "Geometry for the selfish herd," *Journal of theoretical Biology*, vol. 31, no. 2, pp. 295–311, 1971.
- [12] G. M. Werner and M. G. Dyer, "Evolution of herding behavior in artificial animals," *from animals to animats*, vol. 2, pp. 393–399, 1993.
- [13] W. Scott and N. E. Leonard, "Pursuit, herding and evasion: A three-agent model of caribou predation," in *2013 American Control Conference*. IEEE, 2013, pp. 2978–2983.
- [14] S. A. Sheded, "Optimal control for a two-player dynamic pursuit evasion game: The herding problem," Ph.D. dissertation, Virginia Polytechnic Institute and State University, 2002.
- [15] P. Kachroo, S. A. Sheded, J. S. Bay, and H. Vanlandingham, "Dynamic programming solution for a class of pursuit evasion problems: the herding problem," *IEEE Transactions on Systems, Man, and Cybernetics, Part C (Applications and Reviews)*, vol. 31, no. 1, pp. 35–41, 2001.
- [16] A. D. Khalafi and M. R. Toroghi, "Capture zone in the herding pursuit evasion games," *Appl. Math. Sci.*, vol. 5, no. 39, pp. 1935–1945, 2011.
- [17] J.-M. Lien, S. Rodriguez, J. Malric, and N. M. Amato, "Shepherding behaviors with multiple shepherds," in *Proceedings of the 2005 IEEE International Conference on Robotics and Automation*. IEEE, 2005, pp. 3402–3407.
- [18] Z. Lu, "Cooperative optimal path planning for herding problems," Ph.D. dissertation, Texas A & M University, 2006.
- [19] A. Pierson and M. Schwager, "Controlling noncooperative herds with robotic herders," *IEEE Transactions on Robotics*, vol. 34, no. 2, pp. 517–525, 2018.
- [20] A. S. Gadre, "Learning strategies in multi-agent systems-applications to the herding problem," Ph.D. dissertation, Virginia Tech, 2001.
- [21] M. Bacon and N. Olgac, "Swarm herding using a region holding sliding mode controller," *Journal of Vibration and Control*, vol. 18, no. 7, pp. 1056–1066, 2012.
- [22] R. A. Licitra, Z. I. Bell, E. A. Doucette, and W. E. Dixon, "Single agent indirect herding of multiple targets: A switched adaptive control approach," *IEEE Control Systems Letters*, vol. 2, no. 1, pp. 127–132, 2017.
- [23] R. A. Licitra, Z. I. Bell, and W. E. Dixon, "Single-agent indirect herding of multiple targets with uncertain dynamics," *IEEE Transactions on Robotics*, vol. 35, no. 4, pp. 847–860, 2019.
- [24] R. A. Licitra, Z. D. Hutcheson, E. A. Doucette, and W. E. Dixon, "Single agent herding of n-agents: A switched systems approach," *IFAC-PapersOnLine*, vol. 50, no. 1, pp. 14 374–14 379, 2017.
- [25] M. Abramowitz and I. A. Stegun, *Handbook of mathematical functions with formulas, graphs, and mathematical tables*. US Government printing office, 1968, vol. 55.
- [26] H. Khalil, *Nonlinear Systems*, ser. Pearson Education. Prentice Hall, 2002. [Online]. Available: https://books.google.co.in/books?id=t_d1IQgAACAAJ
- [27] E. Davison and E. Kurak, "A computational method for determining quadratic lyapunov functions for non-linear systems," *Automatica*, vol. 7, no. 5, pp. 627–636, 1971.
- [28] "<https://in.mathworks.com/help/optim/ug/fmincon.html>"